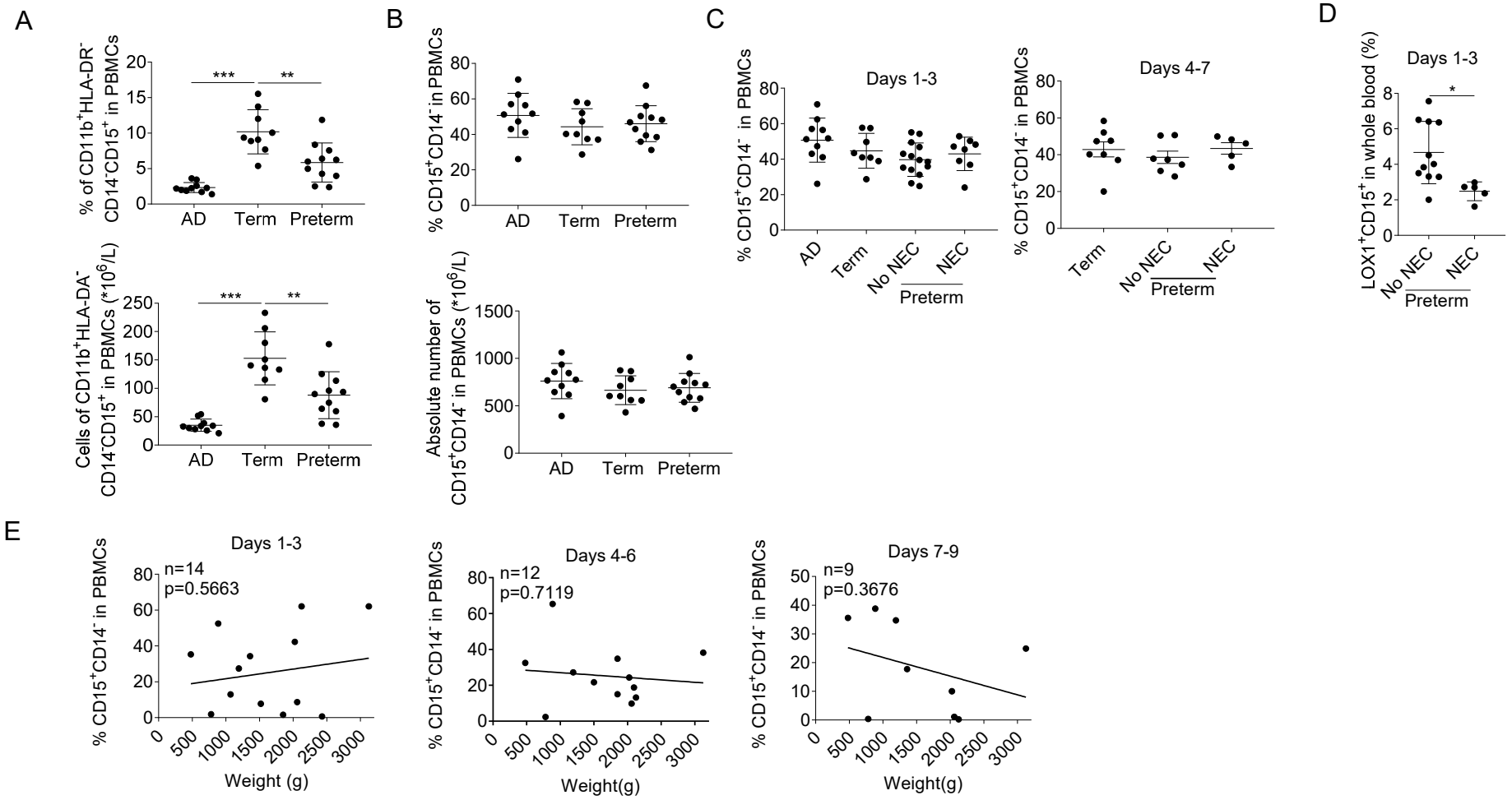

Supplemental Figure 1. MDSC in newborn infants. A. Percentage and absolute numbers of PMN-MDSCs ($CD11b^+HLA\text{-}DR^{-/lo}CD15^+CD14^-$) in AD (adult, n=10) or full term (n=9) and preterm (n=11) infants were analyzed by flow cytometry. B. The percentage and absolute numbers of neutrophils ($CD15^+CD14^-$) in AD (n=10) or full term (n=9) and preterm (n=11) infants were analyzed by flow cytometry. C. Percentage of PMN in adults, full term and preterm infants who either developed or not developed into NEC later. Samples were collected at either day 1-3 (left) or day 4-7 (right) after birth (n=5-14). The results of individual experiments and mean ± SD are shown. D. PMN-MDSCs in samples from infants with birth weight 1,700-2,000 g and gestational age 31-34 weeks collected at days 1-3 after birth. No NEC infants that did not developed NEC (n=11), NEC – infants that developed NEC (n=5). E. Correlation between total neutrophils ($CD15^+CD14^-$) levels and body weight of infants with different ages. In all plots, the results of individual experiments and mean ± SD are shown. P values were calculated in two-sided Student' s *t* tests (D) or 1-way ANOVA followed by Tukey-Kramer multiple-comparisons test (A-C). *-p<0.05; **-p<0.01; ***-p<0.001.

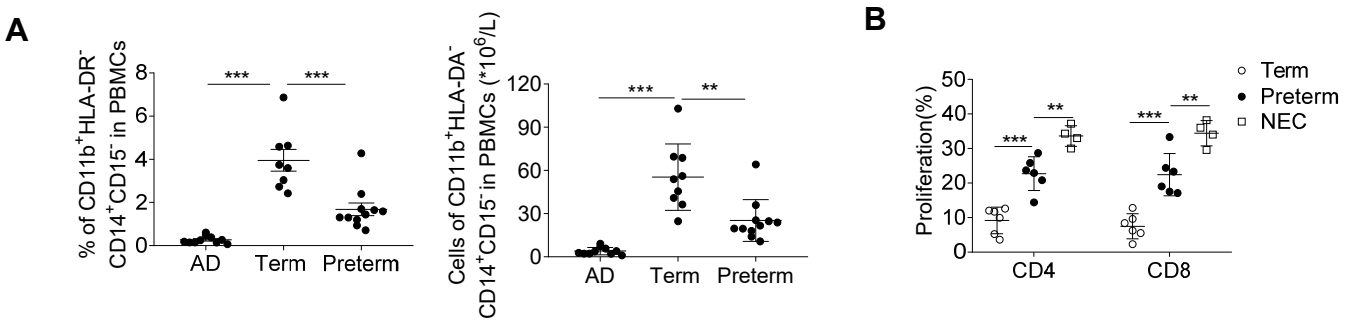

Supplemental Figure 2. M-MDSC in newborn infants. A. Percentage and absolute numbers of M-MDSCs ($CD11b^{+}HLA\text{-}DR^{-/lo}CD14^{+}CD15^{-}$) in AD (n=10), full term (n=8) and preterm (n=11) infants were analyzed by flow cytometry. B. Functional activity of MDSCs from infants. M-MDSCs were sorted from PBMCs of term (n=6), preterm (n=6) and NEC (n=4) infants, followed by coculture with T cells stimulated with anti-CD3/CD28 antibodies. T cell proliferation was measured in triplicate by CFSE labeling. In all plots, the results of individual experiments and mean ± SD are shown. P values were calculated 1-way ANOVA followed by Tukey-Kramer multiple-comparisons test. **-$p<0.01$; ***-$p<0.001$.

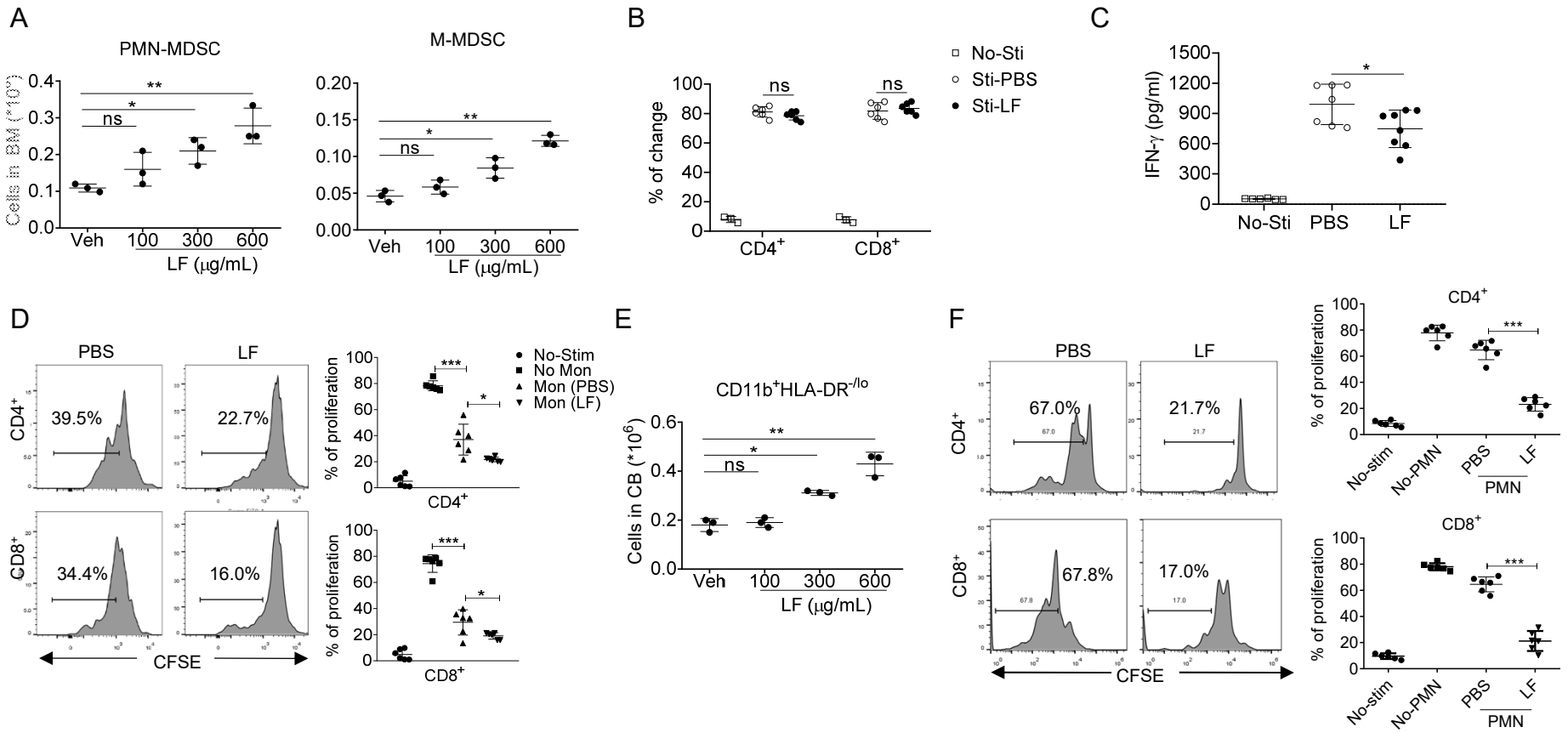

Supplemental Figure 3. The effect of LF on myeloid cells and lymphoid cells. A. BM cells from two-week old mice were treated with different concentrations of LF for 48hr, the absolute numbers of PMN-MDSCs and M-MDSCs were analyzed by flow cytometry. B-C. $CD3^+$ T cells were isolated from WT spleen, after labelling with CSFE, these cells were cultured in the presence of LF (500 μg/mL) or PBS. T cell proliferation (B) and production of IFN-γ (C) were measured after 72 hr stimulation with anti-CD3/CD28 antibodies. D. LF-induced M-MDSC suppression of CD3/CD28-stimulated proliferation of CD4+ and CD8+ T cells. Proliferation was measured by CFSE dilution. Typical example of flow cytometry and cumulative results of mean ± SD (n=6) are shown. Not-stimulated T cells (No-stim) and stimulated T cells without Mon (No-Mon) were used as controls. E. Cord blood (CB) mononuclear cells were treated with different concentrations of LF for 48hr, the absolute numbers of myeloid cells were analyzed by flow cytometry. F. PMN isolated from CB were treated with PBS and LF for 48 hr in the presence of GM-CSF and then added to CD3/CD28 activated T cells. T cells proliferation was measured in triplicates using CFSE dilution. Data represent mean ± SD. P values were calculated 1-way ANOVA followed by Tukey-Kramer multiple-comparisons test. *-$p<0.05$; **-$p<0.01$; ***-$p<0.001$; ns: not significant.

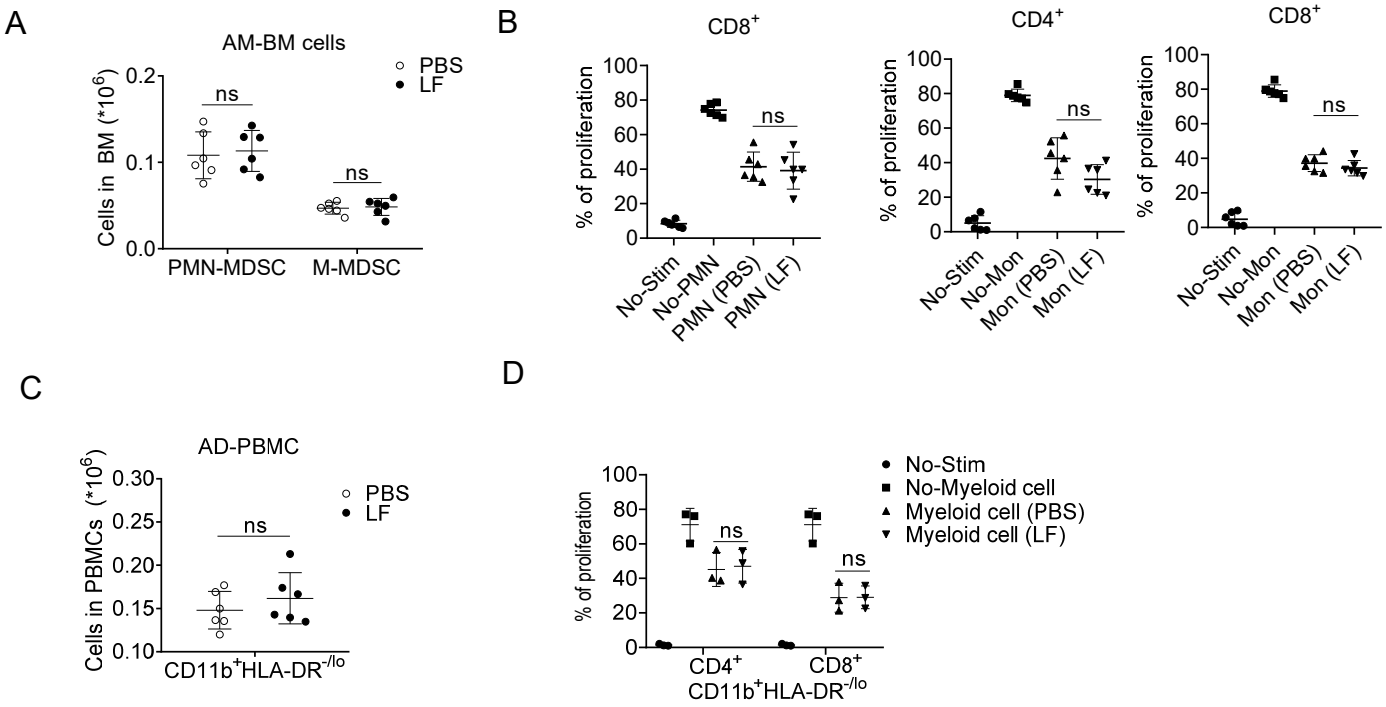

Supplemental Figure 4. LF does not affect myeloid cells from adults. A. BM cells from eight-week-old mice were treated with LF or PBS in the presence of GM-CSF for 2 days. The absolute numbers of PMN-MDSCs and M-MDSCs were analyzed by flow cytometry (*n*=6). B. Left: Antigen-specific proliferation of OT-I-derived $CD8^+$ T cells in the presence of PMN-MDSCs isolated from PBS or LF treated 8-weekold mice BM cells, effectors were stimulated with cognate peptides (SIINFEKL) and proliferation was measured by CFSE dilution. Right, anti-CD3/CD28-inducible proliferation of $CD4^+$ and $CD8^+$ T cells in the presence of M-MDSCs isolated from PBS or LF 8-week-old mice BM cells. No-stim, non-activated T cells (negative control); No-PMN/Mon, activated T cells; T cell proliferation in the presence of PBS (PMN/Mon, PBS) or LF(PMN/Mon, LF) treated MDSCs. Proliferation was measured by CFSE dilution. C. Absolute numbers of myeloid cells ($CD11b^+HLADR^{-/lo}$) in PBS or LF-treated adult PBMC for 2 days were analyzed by flow cytometry (*n* = 6). D. Myeloid cells ($CD11b^+HLA\text{-}DR^{-/lo}$) were sorted from PBS or LF-treated adult PBMC and added to T cells isolated from blood and stimulated with antibodies to anti-CD3/CD28 antibodies. Proliferation was measured in triplicate by CFSE labeling (*n*=3). In all plots, Data represent mean ± SD. P values were calculated in two-sided Student' s *t* tests (A and C) or 1-way ANOVA followed by Tukey-Kramer multiple-comparisons test (B and D-E). ns: not significant.

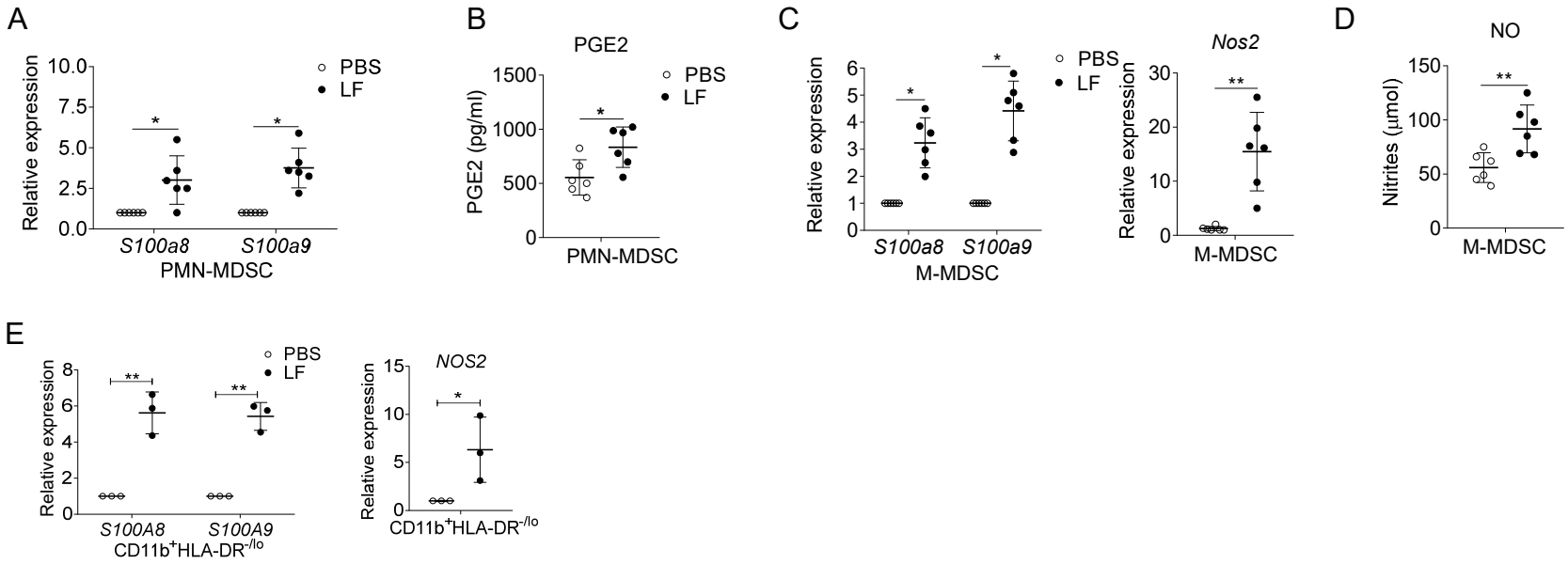

Supplemental Figure 5. Effect of LF on activity of myeloid cells. BM cells from newborn mice were treated with PBS and LF for 48 hr. A. Expression of *S100a8* and *S100a9* in PMN-MDSCs from PBS or LF-treated mouse BM cells were measured by qRT-PCR. B. PGE2 amounts in PMN-MDSCs from PBS or LF-treated mouse BM cells were measured by ELISA. C. Expression of indicated genes in M-MDSCs from PBS or LF-treated mouse BM cells were measured by qRT-PCR. D. NO amounts in M-MDSCs from PBS or LF treated mouse BM cells. E. Expression of indicated genes in myeloid cells from PBS or LF-treated CB mononuclear cells (n=3). In all plots, data represent individual results and mean ± SD (n=3-6 per treatment group). P values were calculated in two sided Student' s *t* tests. *-$p<0.05$; **-$p<0.01$.

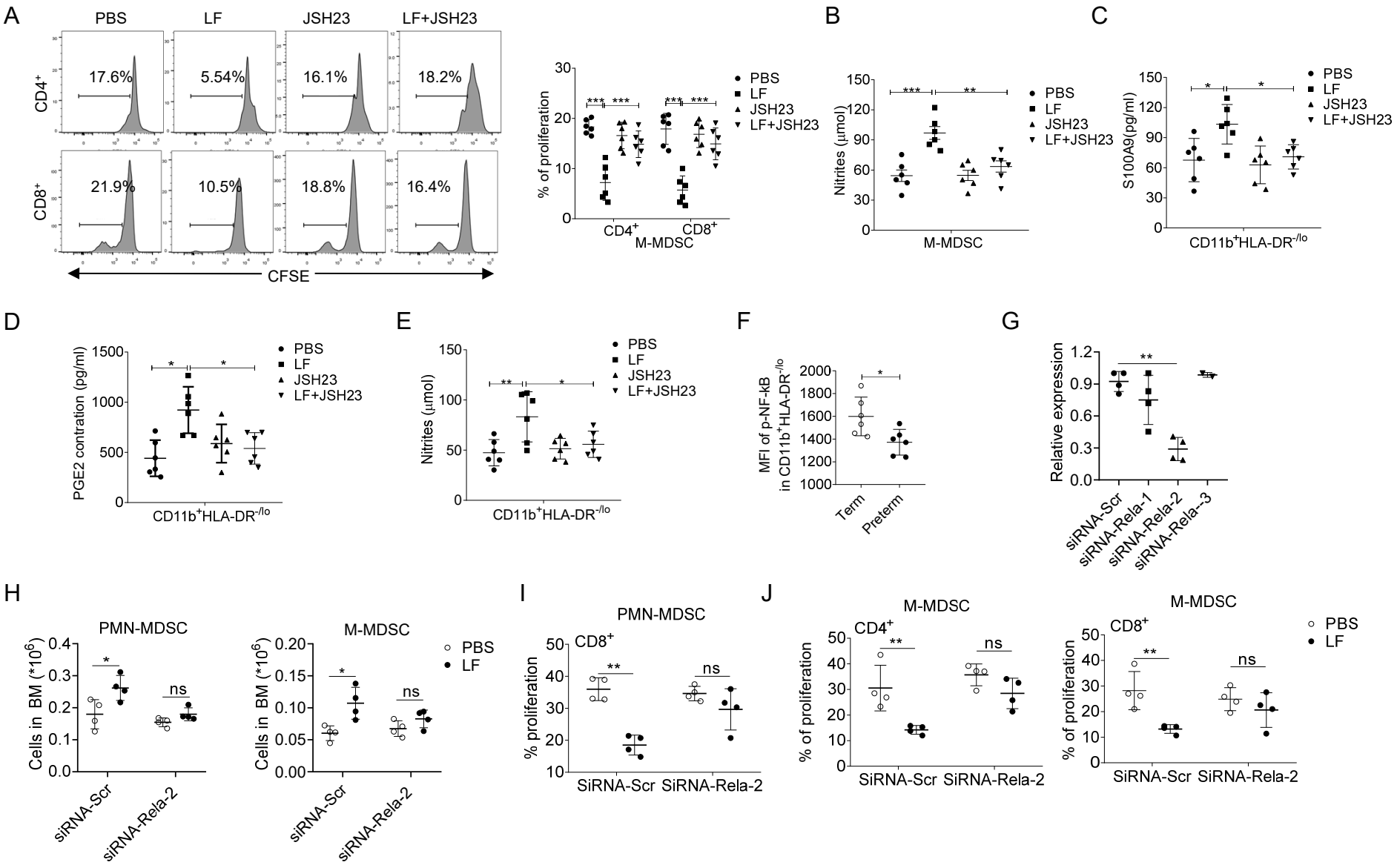
A
PBS
LF
JSH23
LF+JSH23
CD4+
CD8+
17.6%
5.54%
16.1%
18.2%
21.9%
10.5%
18.8%
16.4%
CFSE
% of proliferation
CD4+
CD8+
M-MDSC
PBS
LF
JSH23
LF+JSH23
B
Nitrites (μmol)
M-MDSC
C
S100A9(pg/ml)
CD11b+HLA-DR-/lo
D
PGE2 contration (pg/ml)
CD11b+HLA-DR-/lo
E
Nitrites (μmol)
CD11b+HLA-DR-/lo
F
MFI of p-NF-kB in CD11b+HLA-DR-/lo
Term
Preterm
G
Relative expression
siRNA-Scr
siRNA-Rela-1
siRNA-Rela-2
siRNA-Rela--3
H
PMN-MDSC
M-MDSC
Cells in BM (*10^6)
siRNA-Scr
siRNA-Rela-2
I
PMN-MDSC
CD8+
% proliferation
SiRNA-Scr
SiRNA-Rela-2
J
M-MDSC
CD4+
CD8+
% of proliferation
SiRNA-Scr
SiRNA-Rela-2

Supplemental Figure 6. Effect of NF-kB silencing on myeloid cell response to LF. A. Suppressive activity of M-MDSC. Typical example left panel and cumulative result (right panel). T cells proliferation was measured in triplicate by CFSE staining. For M-MDSCs, effectors were $CD4^+$ or $CD8^+$ T cells stimulated with CD3/CD28 antibodies. Each experiment was performed in triplicates. B. The amount of nitrites in M-MDSCs measured by Nitrite Assay Kit (n=6). C. The amount of S100A9 protein in myeloid cells from LF treated human CB cells (n=6). D. The amount of PGE2 in myeloid cells from LF treated CB cells (n=6). E. The amount of nitrites in myeloid cells from LF treated CB cells (n=6). F. Phosphorylated p65 in myeloid cells from full term and preterm infants analyzed by flow cytometry (n=6). G. BM cells from 2-week old mice were transfected with different siRNA-specific-p65 (RelA) or scramble shRNA (scr). The effect of silencing was confirmed by qRT-PCR and p65-2 siRNA was used in further experiments. H. Mouse BM cells were transfected with siRNA-p65-2 or siRNA-scr, followed by treatment with PBS or LF for 2 days. The absolute numbers of PMN-MDSCs and M-MDSCs were measured by flow cytometry. J. Suppressive activity of PMN-MDSCs (I) and M-MDSCs (J) were measured by CFSE staining. I. $CD8^+$ - splenocytes from OT-1 mice were stimulated with cognate peptide (SIINFEKL). J. $CD4^+$ and $CD8^+$ T cells form C57BL/6 mice were stimulated with CD3/CD28 antibodies. H-J, n=4 In all plots, data represent individual results and mean ± SD. P values were calculated in two-sided Student' s *t* tests (**F** and **H-J**) or 1-way ANOVA followed by Tukey-Kramer multiple-comparisons test (**A-E** and **G**). *-$p<0.05$; **-$p<0.01$; ***-$p<0.001$; ns: not significant..

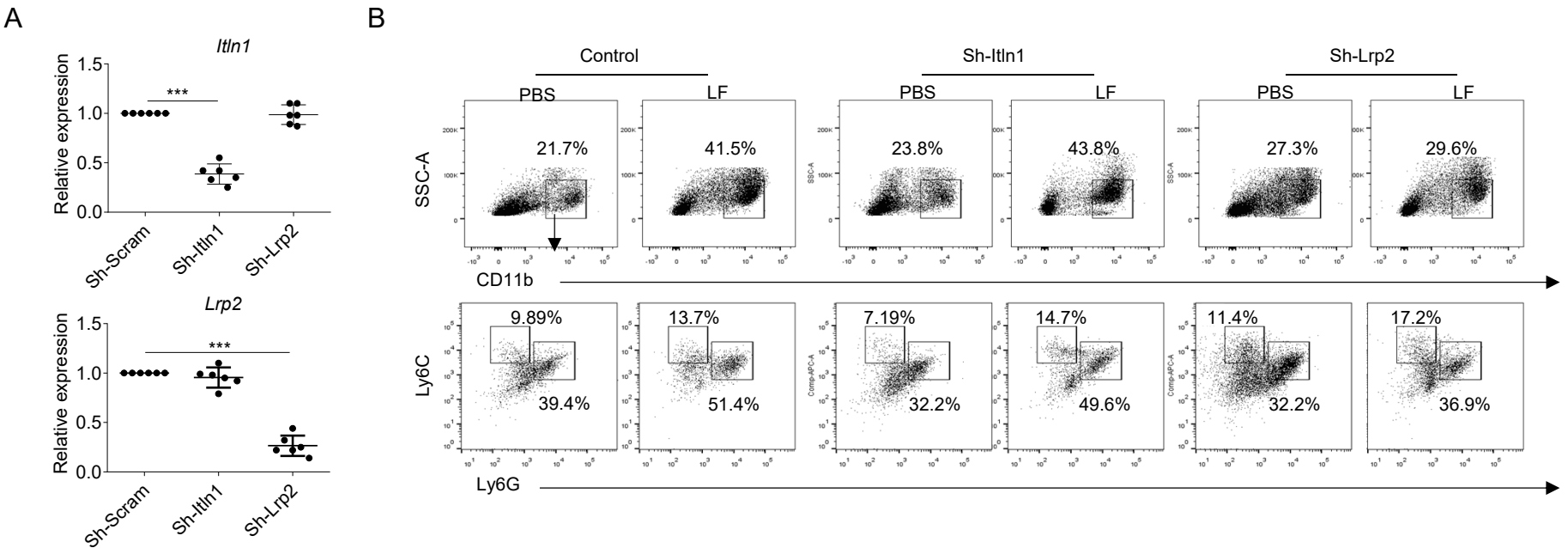

Supplemental Figure 7. Silencing of *Lrp2* and *Itln1*. A. Silencing of *Itln1* and *Lrp2* genes in BM cells from 2-week-old mice were performed by infection with lentiviruses contains *Itln1* and *Lrp2*-specific short hairpin (sh) RNA or scramble shRNA (control), the effect of silencing was confirmed by qRT-PCR (n=6). B. Representative flow cytometric analysis of MDSCs in *Itln1*, *Lrp2*-specific shRNA or scramble shRNA (control) infected BM cells. Transduced GFP+ cells were first gated. P values were calculated in 1-way ANOVA followed by Tukey-Kramer multiple-comparisons test. ***-$p<0.001$.

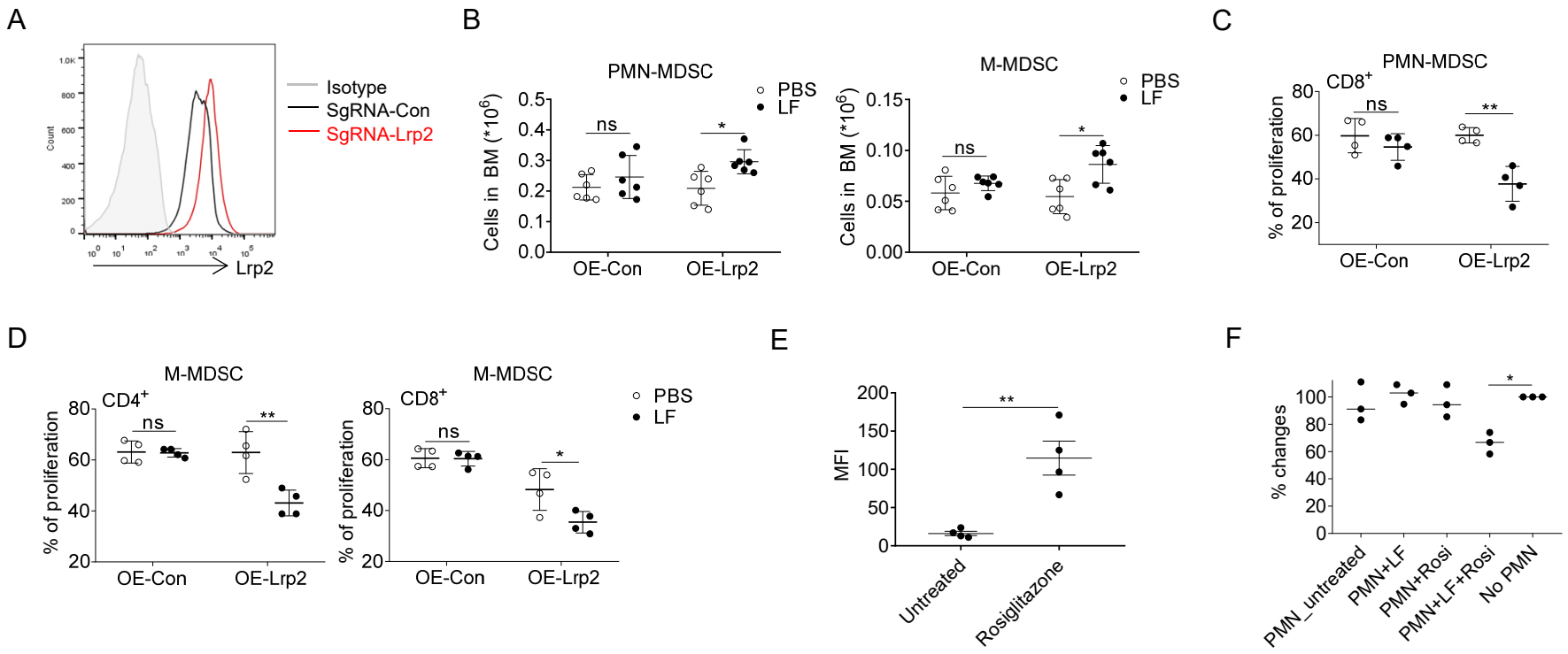

Supplemental Figure 8. Effect of Lrp2 overexpression on myeloid cell response to LF. Lrp2 was overexpressed in adult (6-8 weeks old) mouse BM cells using lentiSAMv2-sgRNA-Lrp2. In control, lentivirus without sgRNA was used. A. Expression of Lrp-2 protein (OE-Lrp2) by flow cytometry. Control – no sgRNA lentivirus (OE-con). B. BM cells were treated with PBS or LF for 2 days. The absolute numbers of PMN-MDSCs and M-MDSCs were measured by flow cytometry. C-D. Suppressive activity of PMN-MDSCs (C) and M-MDSCs (D) was measured using CFSE staining against $CD8^+$ OT-1 T cells stimulated with cognate peptide (for PMN-MDSC) or $CD4^+$ and $CD8^+$ T cells stimulated with CD3/CD8 antibody (for M-MDSC). In all plots, data represent mean ± SD from 4-6 samples per treatment group. E. BM cells from adult mice were treated with 2 mM Rosiglitazone overnight. Lrp2 expression in $CD11b^+Ly6C^{lo}Ly6G^+$ PMN was measured (n=4). F. PMN were treated with 2 mM Rosiglitazone and 700 µg/ml LF overnight and then used to suppress response of OT-1 splenocytes to cognate peptide (SIINFEKL). Cell proliferation was measured in triplicates by ^{3}H-thymidine uptake. Three experiments were performed. Percentage of change of proliferation from no PMN group is shown. P values were calculated in two-sided Student' s t tests (**B-E**) or 1-way ANOVA followed by Tukey-Kramer multiple-comparisons test (**F**). *-$p<0.05$; **-$p<0.01$; ns: not significant.

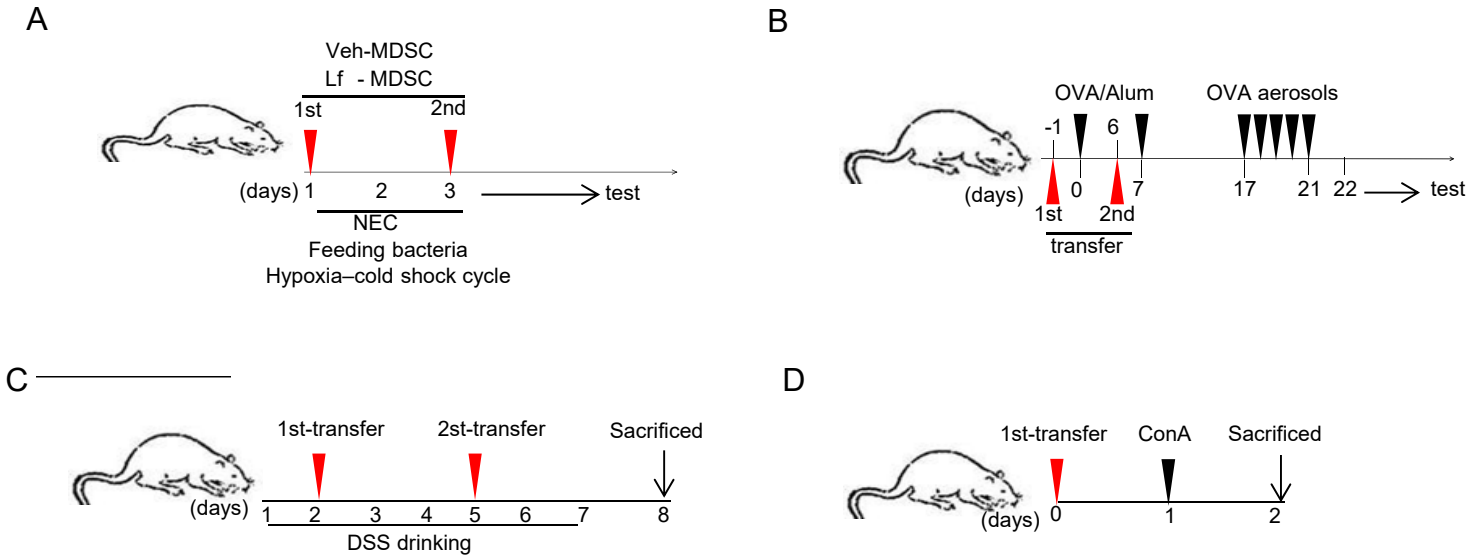

Supplemental Figure 9. The experimental schemas of murine inflammatory diseases. A. Experimental schema of NEC development. 1-3 day old mice were induced with NEC by gavage/hypoxia procedures. One million $Gr1^{+}CD11b^{+}$cells from PBS or LF-treated BM from newborn mice were injected *i.p.* into NEC mice at day 1 and day 3 after disease induction. B. Experimental schema of OVA-induced lung inflammation. Adult mice (6-8 weeks) were sensitized and challenged intranasal with OVA. One million $Gr1^{+}CD11b^{+}$cells from PBS or LF treated BM from newborn mice were injected *i.p.* C. Experimental schema of DSS-induced colitis. Adult mice (6-8 weeks) received 2.5% (w/v) DSS (MP Biomedicals) ad libitum in drinking water for 7 days to induce colitis. One million $Gr\text{-}1^{+}CD11b^{+}$ cells from PBS or LF-treated BM from newborn mice were injected *i.p.* D. Experimental scheme of Con A-induced hepatitis. One million $Gr1^{+}CD11b^{+}$cells from PBS or LF treated BM from newborn mice were injected *i.p.* into adult mice (6-8 weeks) at day 0. Mice were treated with a single intravenous injection of Con A (Sigma-Aldrich, St. Louis, MO) at dose of 20 mg/kg body weight at day 1 and were sacrificed 24 h after Con A administration.

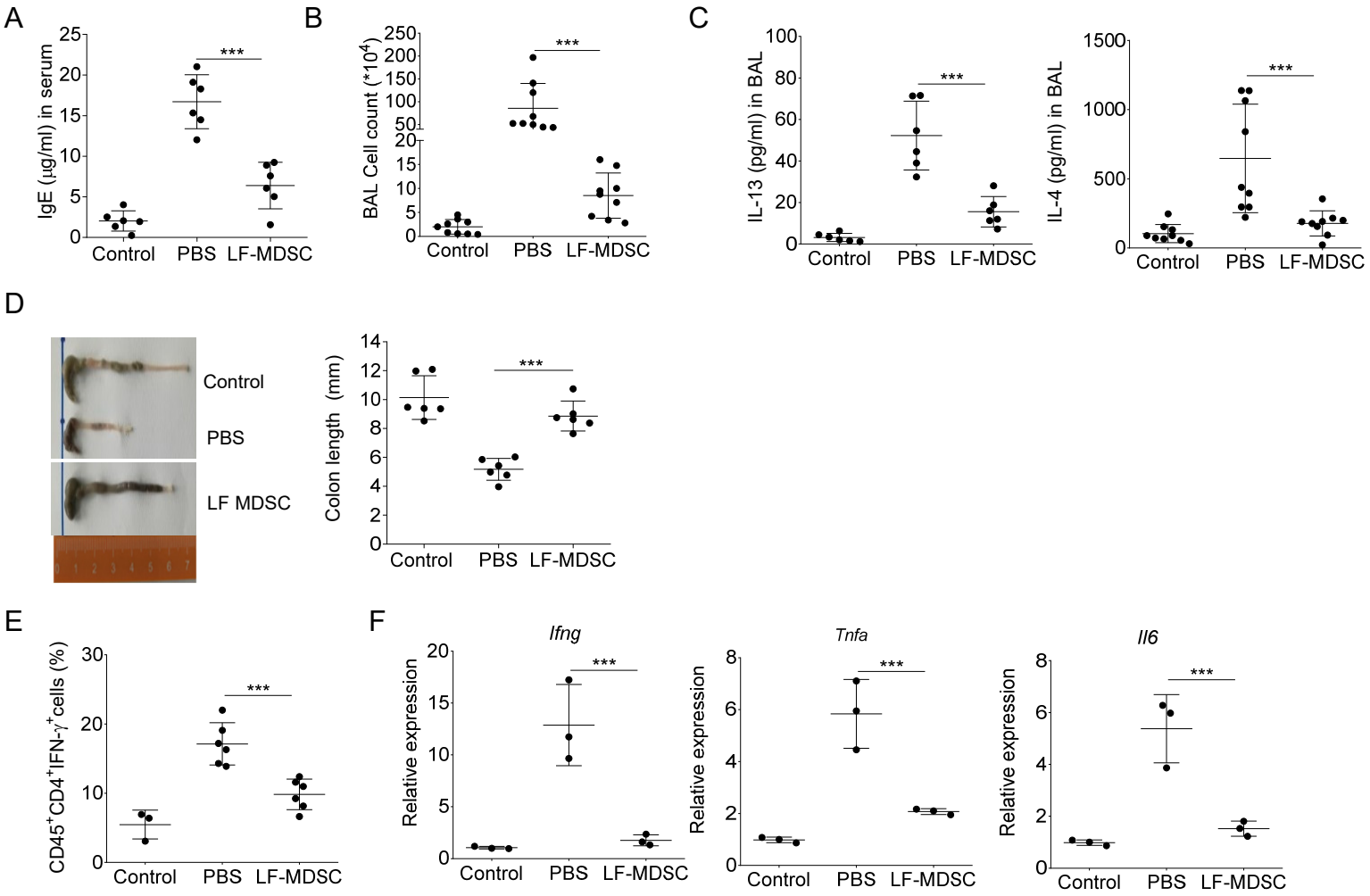

Supplemental Figure 10. Therapeutic effect of LF-MDSC in inflammatory conditions. A-C. Lung inflammation induced by OVA in 6-8 weeks adult mice. A. The amounts of IgE in serum after lung inflammation induction with or without transfer of exogenous LF-derived MDSCs measured by ELISA (n=6). B. The total cell count in bronchoalveolar lavage (BAL) (n=9). C. IL-13 (left) and IL-4 (right) in BAL measured by ELISA (n=6-9). D. DSS induced model of colitis in 6-8 weeks adult mice. The colon length was indicated (D). E-F. The model of ConA-induced hepatitis in 6-8 weeks adult mice. E. The numbers of IFN-γ producing CD4+ T cells in liver after hepatitis induction with or without transfer of exogenous LF-derived MDSCs (n=3-6). F. Expression of *Ifng, Tnfa* and *Il6* genes in liver tissues after hepatitis induction with or without transfer of exogenous LF-derived MDSC (n=3). Data represent individual results and mean ± SD. P values were calculated in 1-way ANOVA followed by Tukey-Kramer multiple-comparisons test. ***-p<0.001.

Supplementary Table S1. Clinical characteristics of infants

Sun Yet Sen University, Guangzhou, China

Characteristic	Term	Preterm		NEC
		No NEC	NEC	
No. of subjects	17	66	14	14
Age(days)	4.3±1.8	2.2±2.2	2.5±2.9	11.6±7.6
Gender(M:F)	8:9	19:41	8:6	4:10
Body weight(kg)	3.18±0.44	2.12±0.48	1.69±0.38	1.35±0.66
Gestational age(week)	37.8±0.9	34.4±1.9	32.0±2.0	34.6±1.88
Antenatal steroids, n (%)	0(0%)	23(34.8%)	9(64.3%)	12(85.7%)
Other diseases				
Feeding intolerance, n (%)	0(0%)	8(12.1%)	2(14.3%)	3(21.4%)
Respiratory distress syndrome, n (%)	0(0%)	23(34.8%)	5(35.7%)	9(64.2%)
Neonatal infection, n (%)	0(0%)	11(16.7%)	7(50%)	3(21.4%)
Neonatal anemia, n (%)	0(0%)	23(34.8%)	10(71.4%)	10(71.4)

Children's Hospital of Philadelphia, USA

Characteristic	Term	Preterm	
		No NEC	NEC
No. of subjects	2	22	8
Gender(M:F)	2:0	11:11	6:2
Body weight(kg)	2.78±0.49	1.42±0.48	0.98±0.33
Gestational age(week)	38.6±1.7	30.2±2.9	26.7±2.1
Antenatal steroids, n (%)	0(0%)	13(59.1%)	8(100%)
Other diseases			
Feeding intolerance, n (%)	0(0%)	4(18.2%)	8(100%)
Respiratory distress syndrome, n (%)	0(0%)	17(77.3%)	8(100%)
Neonatal infection, n (%)	0(0%)	1(4.55%)	4(50%)
Neonatal anemia, n (%)	0(0%)	6(27.3%)	8(100%)

Supplementary Table S2. Reagents

Name	Company	Name	Company
RPMI 1640	Invitrogen	Si-m-Rela_003 (siB08421165612)	Ribobio
CFSE	Invitrogen	siR NC #1(Scramble, siN0000001)	Ribobio
LF (Lactoferrin) , L9507	Sigma-Aldrich	Recombinant murine GM-CSF	R&D
FBS	Invitrogen	Recombinant human GM-CSF	R&D
TRIzol reagent	Invitrogen	Human LTF ELISA kit (RAB0705)	Sigma-Aldrich
Ficoll	GE	Mouse IL4-ELISA Kit (M4000B)	R&D
Nitrite Assay Kit (Griess Reagent) (K544-200)	Biovision, Milpitas, CA	Mouse IgE ELISA Kit (EMIGHE)	Invitrogen
DSS	MP Biomedicals	Human PGE2 ELISA kit (KHL1701)	Invitrogen
ConA (C2272)	Sigma-Aldrich	Mouse PGE2 ELISA kit (KGE004B)	R&D
SIINFEKL, S7951	Sigma-Aldrich	Mouse IL13 ELISA Kit (Catalog:BMS6015)	Invitrogen
Ovalbumin	Sigma-Aldrich	Human S100A9 ELISA kit (ab222271)	Abcam
JSH-23 (S7351)	Selleck	Mouse S100A9 ELISA kit (ab213887)	Abcam
Fluorescein isothiocyanate–dextran (FD70)	Sigma-Aldrich	LRP2 Polyclonal Antibody Catalog # PA5-67900	Invitrogen
Imject™ Alum Adjuvant (77161)	Thermo Scientific	ITLN1 Polyclonal Antibody (Catalog # PA5-42037)	Invitrogen
pHrodo™ Green Zymosan Bioparticles™ Conjugate for Phagocytosis (P35365)	Invitrogen	Phospho-NF-κB p65 (Ser536) (93H1, #3033)	Cell Signaling Technology
Candida albicans (Robin) Berkhout (ATCC® 10231™)	ATCC	Anti-Histone H3 (ab12209)	Abcam
Escherichia coli (Migula) Castellani and Chalmers (ATCC® 12435™)	ATCC	Anti-beta Actin (ab8226)	Abcam
Si-m-Rela_001 (siB08421165522)	Ribobio	Goat anti-Rabbit IgG (H+L) Highly Cross-Adsorbed Secondary Antibody, Alexa Fluor Plus 647, A32733	Invitrogen
Si-m-Rela_002 (siB08421165555)	Ribobio	Rabbit IgG Isotype Control (SP137)	Invitrogen

Supplementary Table S3. Antibodies

Name	Clone	Company	Name	Clone	Company
anti-mouse CD3 functional grade	145-2C11	eBioscience	anti-human CD3 functional grade	HIT3a	eBioscience
anti-mouse CD28 functional grade	37.51	eBioscience	anti-human CD28 functional grade	CD28.2	eBioscience
anti-mouse CD11b-FITC/PerCP-Cy5.5	M1/70.15	eBioscience	anti-human CD11b-FITC	M1/70	eBioscience
anti-mouse Ly6C-PerCP-Cy5.5/APC	HK1.4	ebioscience	anti-human HLA-DR-APC	LN3	eBioscience
anti-mouse Ly6G-PE/FITC	1A8	BD Biosciences	anti-human CD14-PE-cy7/PerCP-Cy5.5	61D3	eBioscience
anti-mouse Gr-1-PE-Cy7	RB6-8C5	BD Biosciences	anti-human CD15-PE	HI98	eBioscience
anti-mouse CD3e-PE	145-2C11	eBioscience	anti-human CD3-PE	UCHT1	eBioscience
anti-mouse CD4-PE-cy7	GK1.5	eBioscience	anti-human CD4-PE	MHCD0404	eBioscience
Anti-mouse CD8-PE	53-6.7	eBioscience	anti-human CD8-PE-Cy7	RPA-T8	eBioscience
Anti-Fc receptor blocking antibody (anti-CD16/CD32) (Catalog # 14-0161-81)	93	Invitrogen	anti-human LOX1-APC	15C4	Biolegend
anti-mouse CD45-PE	30-F11	eBioscience	Si-m-Rela_001	siB08421165522	Ribobio
anti-mouse IFN-ɣ-APC	XMG1.2	eBioscience	Si-m-Rela_002	siB08421165555	Ribobio
anti-mouse CCR3-APC	J073E5	Biolegend	Si-m-Rela_003	siB08421165612	Ribobio
			siR NC #1(Scramble),	siN0000001	Ribobio

Supplementary Table S4. Primer sequences

Primers name	Sequence	Primers name	Sequence
Ms-Actb-for	5'-CGTGCGTGACATCAAAGAGAAG-3'	Hu-ARG1-for	5'-GTGGAAACTTGCATGGACAAC-3'
Ms-Actb-rev	5'-CGTTGCCAATAGTGATGACCTG-3'	Hu-ARG1-rev	5'-AATCCTGGCACATCGGGAATC-3'
Ms-Nos2-for	5'-CACCTTGGAAGAGGAGCAAC-3'	Hu-ITLN1-for	5′-ACGTGCCCAATAAGTCCCC-3′
Ms-Nos2-rev	5'-AAGGCCAAACACAGCATACC-3'	Hu-ITLN1-rev	5′-CCGTTGTCAGTCCAACACTTTC-3′
Ms-S100a8-for	5'-GGAAATCACCATGCCCTCT-3'	Hu-ITLN2-for	5′-AGCCATACCTGTGGTCTATGA-3′
Ms-S100a8-rev	5'-TTTATCACCATCGCAAGGAAC-3'	Hu-ITLN2-rev	5′-CCTGCAACAAATTCCCGTTGA-3′
Ms-S100a9-for	5'-AATGGTGGAAGCACAGTTGG-3'	Hu-LRP1-for	5′-ATCCCAAAGGTGGAACGC-3′
Ms-S100a9-rev	5'-GCTGATTGTCCTGGTTTGTG-3'	Hu-LRP1-rev	5′-CGTGATGCCATGAGGAAA-3′
Ms-Ifng-for	5'-ATA TCT TGG CTT TTC AGC TC -3'	Hu-LRP2-for	5′-CTATGCTACCAATCCGTGTA-3′
Ms-Ifng-rev	5'-CTC CTT TTT CGC TTC CCT GT-3'	Hu-LRP2-rev	5′-AACCCAAACCATCATTATCT-3′
Ms-Tnfa-for	5'-ATCGGTCCCCAAAGGGATGAGAAGTTC-3'	16s UniF340	5'-ACTCCTACGGGAGGCAGCAGT-3'
Ms-Tnfa-rev	5'-GACGTGGGCTACAGGCTTGTCACTC-3'	16s UniR514	5'-ATTACCGCGGCTGCTGGC-3
Ms-Il6-for	5'-CTGCAAGAGACTTCCATCCAG-3	Sg-Lrp2-1-F:	CACCG**ACCGCCCCGGAACTAGCATG**
Ms-Il6-rev	5'-AGTGGTATAGACAGGTCTGTTGG-3	Sg-Lrp2-1-R:	AAACCA**TGCTAGTTCCGGGGCGGT**C
Ms-Itln1-for	5′-TGACAATGGTCCAGCATTACC-3′	Sg-Lrp2-2-F:	CACCGA**CTAGCATGCGGGAATCCAG**
Ms-Itln1-rev	5′-ACGGGGTTACCTTCTGGGA-3′	Sg-Lrp2-2-R:	AAAC**CTGGATTCCCGCATGCTAGT**C
Ms-Itlnb-for	5′-GCGCTTGGGCCATAATCTGT-3′	Sg-Lrp2-3-F:	CACCG**CCCGCATGCTAGTTCCGGGG**
Ms-Itlnb-rev	5′-CGGCCAGAGGGAGAGTAATAA-3′	Sg-Lrp2-3-R:	AAAC**CCCCGGAACTAGCATGCGGG**C
Ms-Lrp1-for	5′-GAGTGTTCCGTGTATGGCAC-3′	Sg-Lrp2-4-F:	CACCG**CCAGAGTCGCAAAGTGCAGG**
Ms-Lrp1-rev	5′-GATGCCTTGGATGATGGTC-3′	Sg-Lrp2-4-R:	AAAC**CCTGCACTTTGCGACTCTGG**C
Ms-Lrp2-for	5′-CGTGCCTACCTTCCCGAC-3′	Sg-Lrp2-5-F:	CACC**GCCCTCTAGACCAGACCGCCC**
Ms-Lrp2-rev	5′-CGGACTTGAGTGAGCCAGG-3′	Sg-Lrp2-5-R:	AAAC**GGGCGGTCTGGTCTAGAGGG**C
Hu-ACTB-for	5'-CTCCATCCTGGCCTCGCTGT-3'	Sg-Lrp2-6-F:	CACCG**CCGCCCCGGAACTAGCATGC**
Hu-ACTB-rev	5'-GCTGTCACCTTCACCGTTCC-3'	Sg-Lrp2-6-R:	AAAC**GCATGCTAGTTCCGGGGCGG**C
Hu-S100A8-for	5'-CCCTGATAAAGGGGAATTTCCATGC-3'	Lrp2-shRNA-1	Dharmacon, Cat#:TRCN0000240612
Hu-S100A8-rev	5'-CTGGAAGTTAACTGCACCATCAGTG-3'	Lrp2-shRNA-2	Dharmacon, Cat#:TRCN0000240609
Hu-S100A9-for	5'-ATCATCAACACCTTCCACCA-3'	Itln1-shRNA-1	Dharmacon, Cat#:TRCN0000324326
Hu-S100A9-rev	5'-GCTTGTCTGCATTTGTGTCC-3'	Itln1-shRNA-2	Dharmacon, Cat#:TRCN0000353857
Hu-NOS2-for	5'-GGCCTGTCCTTGGAAATTTCTGTTC-3'		
Hu-NOS2-rev	5'-GCTGAGGTTGTGATACTGAAGGTCA-3'		